Extended x-ray-absorption fine-structure study of Ag particles isolated in solid argon

P. A. Montano
Department of Physics, West Virginia University, Morgantown, West Virginia 26506-6023

W. Schulze and B. Tesche
Fritz-Haber-Institut der Max-Planck-Gesellschaft, Faradayweg 4-6, D-1000 Berlin 33/Dahlem, Germany

G. K. Shenoy and T. I. Morrison
Argonne National Laboratory, Argonne, Illinois 60439

Extended x-ray-absorption fine structure was used to determine the nearest-neighbor distance for silver particles isolated in solid argon. The silver particles were produced in the gas phase with the use of the gas-aggregation technique. In this technique the metal atoms are evaporated in an argon atmosphere in the pressure range 0.1–10 Torr; a cooling of the metal atoms takes place through collision with cold gas atoms. The metal aggregates are then transported by the gas stream through an aperture into a liquid-helium cryopump, where most of the gas is condensed. The metal flow rate is monitored by a quartz oscillator. The size of the metal clusters can be selected by changing the argon pressure, density of the metal atom vapors, and geometric configuration of the cell. The size distribution was determined by introducing a sample holder into the molecular beam, sampling an atomic quantity of approximately 10^{15} atoms/cm^2, and evaluating the corresponding electron micrographs. Particles with average sizes between 25 and 130 Å were studied. A careful analysis of the data was performed with a thin silver foil at 78 K as a standard. No remarkable effects were observed in the near-edge region of the K edge, but there was a noticeable contraction of the nearest-neighbor distance. This contraction can be explained if we assume the presence of surface stresses. There is good agreement between the observed contraction and the calculated values.

INTRODUCTION

Understanding the physical properties of metal aggregates is of great importance to many fields in solid-state physics and chemistry, including such diverse areas as nucleation, surface chemistry and physics, and heterogeneous[1] catalysis. The most important parameter relating experimental spectroscopic information on clusters to theoretical calculations is the interatomic distance, since variations in such parameters strongly affect the nature of molecular-orbital interactions and bonding of absorbates. Consequently, the determination of the interatomic distance in metal clusters becomes a crucial task. There have been several electron-diffraction studies reported in the literature concerning the variation in the lattice constant of various materials as a function of particle size.[2,3] A contraction of the lattice spacing was observed in some cases, however, a straightforward interpretation of the electron-diffraction data for small particles is rather difficult and may lead to incorrect values for the interatomic distances.[2]

Recently, x-ray-absorption fine-structure (EXAFS) measurements have been used to study the variation of interatomic distances.[4-6] EXAFS measurements in Cu and Ni clusters on carbon substrates have shown a contraction of the interatomic distance for metal clusters with an average diameter of 100 Å or less.[4] Those results markedly contrast with the electron-diffraction observation for Cu small particles performed by Wasserman and Ver-

maak.[3] In the former experiments the metal clusters are produced by evaporation of the metal atoms and deposition on a substrate. The size of the metal clusters is determined by the amount of metal deposited on the substrate. A disadvantage in this procedure is associated with the difficulty of obtaining the size and morphology of the clusters. There is also the added difficulty of substrate interaction with the clusters which could produce noticeable changes for the very small particles. An alternative method is the use of the matrix-isolation technique. By studying small metal aggregates in noble-gas matrices, it is possible to investigate metal-metal interactions without the interference of strongly interacting supports.[7,8] The noble-gas matrix provides a support which is transparent to electromagnetic radiation over a wide energy range, thus facilitating the study of the metal clusters employing a great diversity of techniques. Matrix-isolated metal clusters can be generated in the gas phase and then isolated, or they can be formed in the matrix itself, either during matrix growth[5,7] or by thermal annealing of the matrix. It is to be noted that the weakly interacting supports commonly used in matrix-isolation experiments are unlikely to appreciably disturb the electronic and geometric properties of the isolated clusters.[7-9]

Matrix-isolation techniques in conjunction with EXAFS were successfully used to determine the interatomic distances in Fe dimers[5] and small clusters of iron isolated in solid neon.[6] A considerable contraction in the interatomic distances was observed for the metal mole-

cules as compared to bulk α-Fe. The technique used permitted only the identification of M_2 clusters, and occasionally M_3 and M_4. However, when the metal concentration in the matrix increases, a wide distribution of cluster sizes is obtained. As a result a wide gap exists between the clusters made up of two and three metal atoms and very large clusters (100 Å or more) where no reliable technique has been used to determine interatomic distances. Recently, metal clusters with a narrow size distribution and with an average diameter of less than 100 Å have been successfully prepared using the gas-aggregation technique.[10] In the present paper we report a series of EXAFS measurements on matrix-isolated Ag clusters prepared by the gas-aggregation technique. A contraction in the interatomic distances is observed for the smaller clusters. This contraction can be explained qualitatively and quantitatively in terms of surface stresses.[2,3,11,12] A full description of this work is presented in this paper.

EXPERIMENTAL TECHNIQUES

The metal clusters were prepared using the gas-aggregation technique. In this technique the metal atoms are evaporated in an argon atmosphere in the pressure range 0.1–10 Torr. Through collisions with cold gas atoms, cooling of the metal atoms takes place. The metal clusters are formed within this cell in a region of sufficiently high supersaturation, the extent of this region being strongly dependent on the cell pressure. The metal aggregates are then transported by the gas stream through an aperture into a liquid-helium cryopump, where most of the gas is condensed (Fig. 1). A second aperture on the axis of this pump allows the production of a collimated molecular beam, which is directed onto a high-purity aluminum substrate cooled with liquid helium where the metal clusters are codeposited with argon gas. The metal-flow rate is monitored by a quartz oscillator mounted on a bellows which allows the oscillator to be moved into the beam. The size of the metal-atom clusters can be selected by changing the argon pressure, density of the metal-atom vapors, and geometric configuration of the cell. The size characterization was achieved from electron microscopy. In order to do this, a simple plate mounted on a second bellows was introduced in the path of the molecular beam, sampling an atomic metal quantity of approximately 10^{15} atoms/cm². The sample substrate consisted of an amorphous carbon film 20 Å thick supported by a Cu grid. The particle size was determined
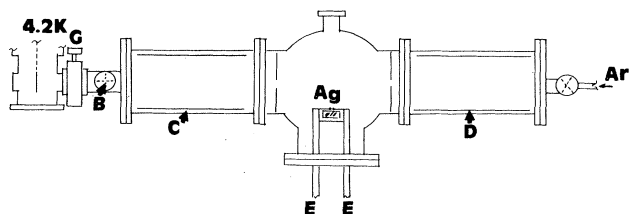
separately in an electron microscope. An example of the histograms of particle-size distribution for the silver clusters is given in Fig. 2. The sample of Ag clusters isolated in argon were deposited in ultrahigh-purity aluminum, with the metal concentration less than 0.5 at. %. The helium cryostat containing the sample could be decoupled from the molecular-beam system by using a gate valve, thus allowing the transfer of the cryostat to the experimental hutch.

All x-ray-absorption spectra were recorded using radiation at the Stanford Synchrotron Radiation Laboratory (SSRL) on beam line I-5. Both transmission and fluorescence measurements were carried out to collect the EXAFS data. Standard ionization chambers filled with argon were used for the detection of the incoming and transmitted beam; a NaI detector was used for detecting the fluorescent x rays. Energy calibration was performed using an ultrahigh-purity Ag foil at 78 K. The derivative of the absorption edge was used to determine the position of the K edge in silver metal (25 516 eV). The K edge of the matrix-isolated species was determined using the same technique. Comparison of calibration spectra before and after the measurements for each sample indicated no shifting of the energy calibration.

The EXAFS can be expressed as[13,14]

$$\chi(k) = \frac{\mu_k(k) - \mu_0(k)}{\mu_0(k)}$$

$$= \frac{1}{k} \sum_b A_b(k) \sin[2kR_b + \alpha_{ab}(k)] , \qquad (1)$$

where k is the wave vector of the ejected photoelectrons given by

$$k = [(E - E_0)2m/\hbar^2]^{1/2}$$

and

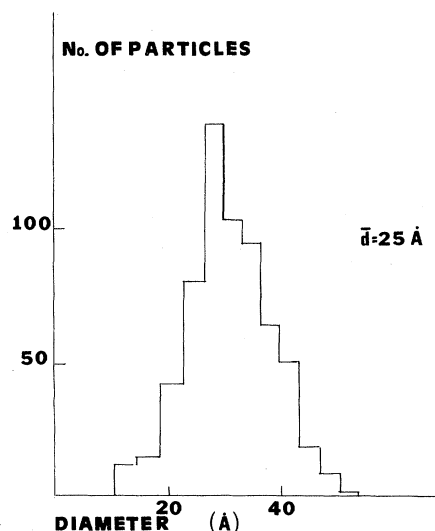$$A_b(k) = \frac{N_b}{R_b^2} |f_b(\pi,k)| \exp[-2\sigma_b^2 k^2 - 2R_b(k)/\lambda(k)] .$$

FIG. 2. Histogram of the particle-size distribution (Y: number of particles; X: particle diameter in Å). $\bar{d}$ is the average particle size.

FIG. 1. Schematic of the system used to prepare the silver clusters. E: electrodes; D: precooling system for the argon; C: liquid-helium cryopump; B: bellows for the quartz oscillator and sample plates for the electronmicroscopy; G: gate valve.

Here $\mu_k(k)$ is the K edge contribution to the absorption coefficient and $\mu_o(k)$ is the smooth background about which μ_k oscillates. In Eq. (1) E is the photon energy, E_0 is the photoelectron threshold energy, N_b is the number of backscattering atoms in the bth shell, σ_b^2 is the mean-square fluctuation in R_b, $|f_b(\pi,k)|$ is the backscattering amplitude for the neighboring atoms, and R_b is the distance from the absorbing atom to the backscattering atoms at the shell b. $\alpha_{ab}(k)$ is an energy-dependent phase shift experienced by an electron leaving the absorbing atom, becoming backscattered, and returning to interfere at the absorbing atom, and $\lambda(k)$ is the mean free path of the ejected photoelectron.

For each sample several measurements were performed (ranging from 10 to 30) until a good signal-to-noise ratio was obtained from the summed data from each measurement. For each transmission spectrum, a Victoreen approximation was fitted to the monotonic preedge and then subtracted to yield $\mu_k(k)$. Cubic polynomials were splined through the oscillation to approximate $\mu_0(k)$ and $\chi(k)$ was calculated using Eq. (1). The analysis of the fluorescence data was performed in a similar manner, although background corrections are simpler to handle in this case. $\chi(k)$ was then multiplied by k^3 to emphasize the higher-k region, where the metal-metal backscattering amplitude is more pronounced. Fourier transforms of the

$k^3\chi(k)$ were performed by choosing the transformation region as bounded by minima in $|\chi(k)|$ and using a Hanning window function that smoothed the ends of the region of zero. This procedure is necessary in order to avoid transform-termination effects. The back transform of the Fourier spectrum was taken using a window over the peak corresponding to the first shell. The resulting spectrum was then analyzed using two methods: Rabe's method[15] of analysis $R = (\alpha_{expt} - \alpha_{AgAg})/2k$ and a nonlinear least-squares fit of the data. The phase shift α_{AgAg} was obtained from the experimental measurements of the silver foil. Both methods gave nearly identical results for the Ag-Ag separation in the matrix-isolated silver clusters of different size.

EXPERIMENTAL RESULTS

The effects near the x-ray-absorption edge structure (XANES) are generally an order of magnitude larger than in the EXAFS region. The near-edge absorption spectra for a Ag foil at 78 K and for silver particles in argon (25 Å average size) are shown in Figs. 3(a) and 4(a), respectively. No significant difference is observed between XANES spectra of metallic silver and the small isolated silver clusters. No appreciable difference in the K-edge position was observed either between metallic silver and
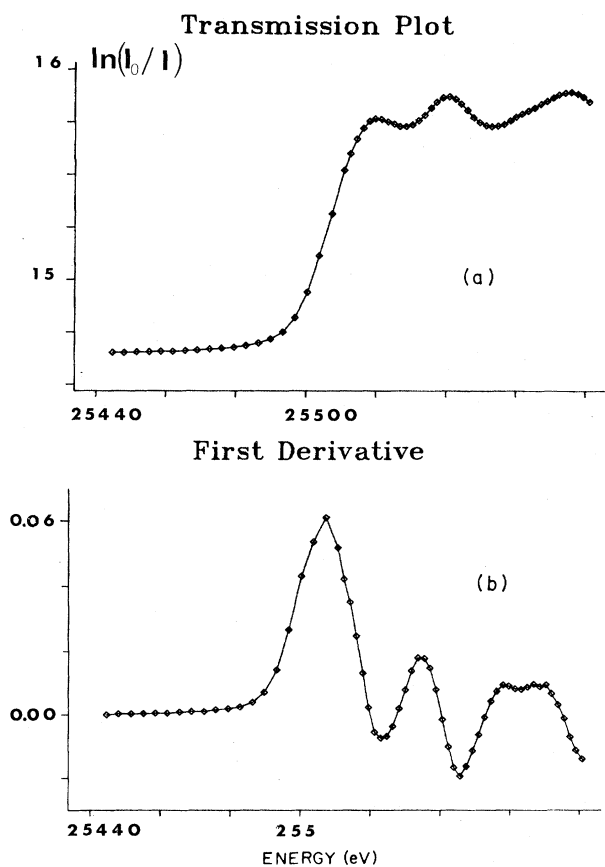

FIG. 3. (a) Near-edge adsorption spectrum of an Ag foil at 78 K. (b) First derivative of the near-edge absorption spectrum of an Ag foil.
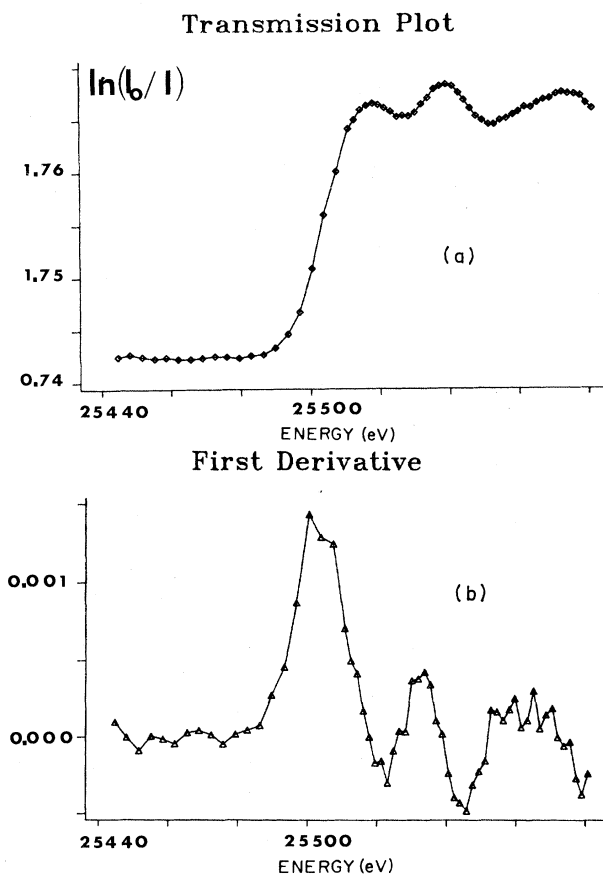

FIG. 4. (a) Near-edge adsorption spectrum of the silver particles in argon ($\bar{d}=25$ Å). (b) First derivative of the near-edge absorption spectrum of the silver particles in argon ($\bar{d}=25$ Å).
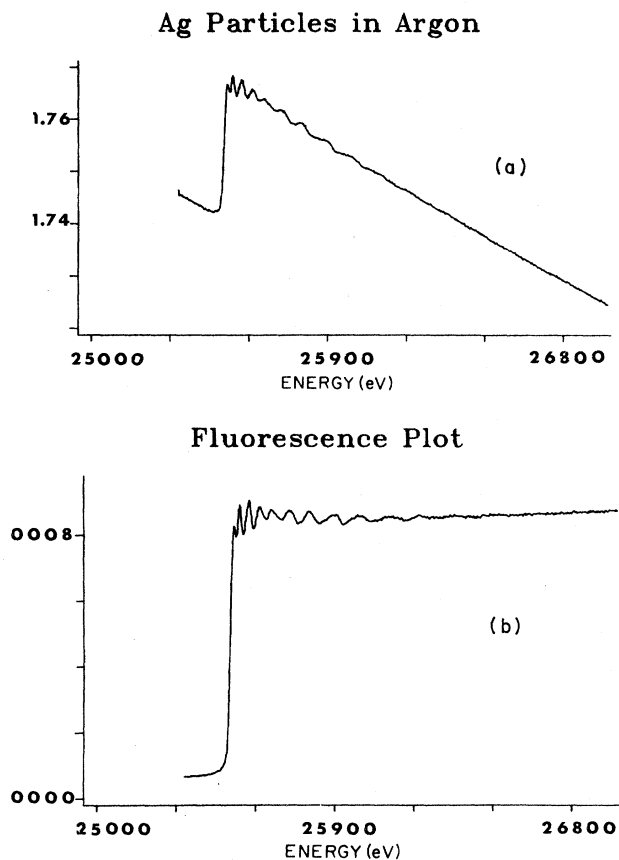
Ag Particles in Argon

(a)

Fluorescence Plot

(b)

FIG. 5. (a) Typical absorption spectrum of the silver particles isolated in argon ($\bar{d}$=25 Å) (raw data) [ln(I_0/I) vs energy]. (b) Typical fluorescence spectrum of the silver particles isolated in argon [$\bar{d}$=25 Å) (raw data) ordinate is I/I_0].

the isolated-metal atom clusters. Figures 3(b) and 4(b) show the first derivative of the near-edge structure of the absorption spectra of the samples in Figs. 3(a) and 4(a). The position of the edge is determined by the first prominent peak in Figs. 3(b) and 4(b). From the present experiments we conclude that down to an average size of 25 Å,
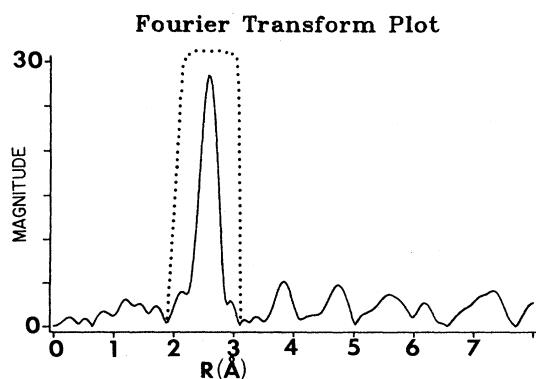
Fourier Transform Plot

FIG. 6. Fourier transform of $k^3\chi(k)$ for the ($\bar{d}$=25 Å) transmission spectrum is shown in this figure. The window for the back transform is indicated in the figure. y axis is in arbitrary units.
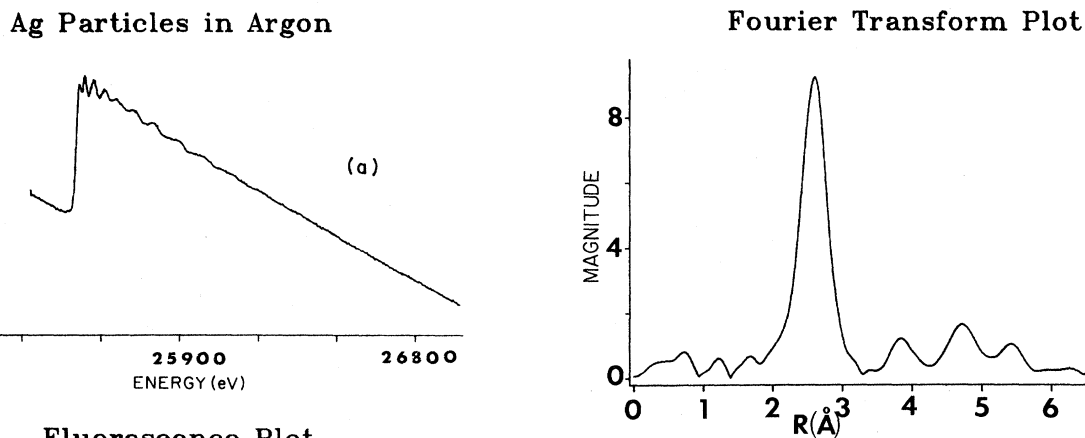
Fourier Transform Plot

FIG. 7. Fourier transform of the silver foil $k^3\chi(k)$. y axis is in arbitrary units.

no significant differences can be observed between the K-edge XANES of small silver particles and silver metal.

The absorption and fluorescence spectra for the whole energy range, shown in Figs. 5(a) and 5(b), respectively, correspond to the sample with the smallest average particle size and are typical of the silver small particles. All the measurements show similar signal-to-noise ratio. The Fourier transform for the $k^3\chi(k)$ spectra of the sample is shown in Fig. 6. For comparison the Fourier transform for the silver foil used as standard (at T=78 K) is shown in Fig. 7. A well-resolved first-shell peak which is easily observed in Fig. 6 will facilitate a highly accurate evaluation of the nearest-neighbor distance for the small metal particles. The presence of peaks due to other shells can be observed in Fig. 6. There are, of course, contributions present from the argon matrix, but only the surface atoms on the silver particles will have argon atoms as neighbors. The window shown in Fig. 6 around the first-shell peak was used to obtain the Fourier back transform (Fig. 8). The nearest-neighbor distance was determined using the experimental phase shift extracted from the silver foil. The same window was used to analyze the foil and the small particle samples. Rabe's method was used to find the nearest-neighbor distance.[15] The data shown in Fig. 8 were also analyzed employing the least-square procedure with Eq. (1). In order to perform the fit, the phase shift obtained from the silver-foil measurements was
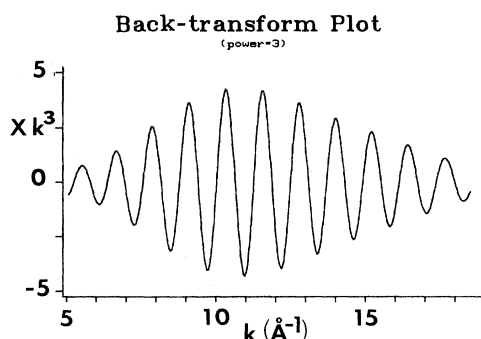
Back-transform Plot
(power=3)

FIG. 8. Back-transform plot of the peak shown in Fig. 6. $k^3\chi(k)$ is the ordinate.
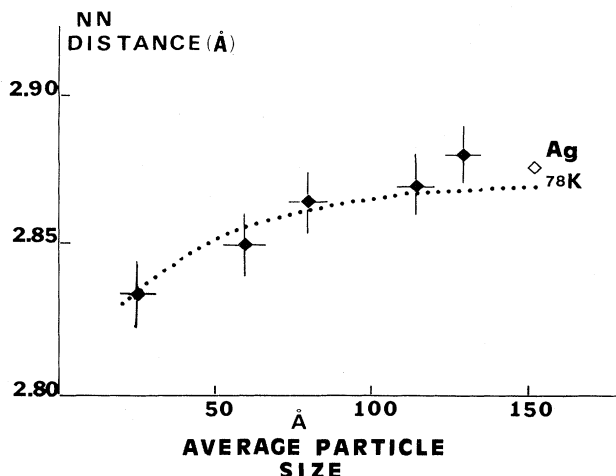
**N N
DISTANCE (Å)**

FIG. 9. Plot of the interatomic distances vs average particle size. Dotted line is the fit using the values of ΔR given by Eq. (4) ($f = 2286$ dyn/cm).

parametrized.[16] The nearest-neighbor distances obtained from the least-squares analysis were identical to those obtained from Rabe's method. Figure 9 shows the plot of the interatomic distance versus average particle size. We observed a small contraction in the interatomic distances for the smaller particles. We also studied two samples that were prepared in the absence of argon in the matrix, by depositing the silver clusters on an Al substrate cooled to 78 K. Although the preparation procedure represented two distinct particle sizes for these samples, the Ag-Ag separation was the same for these samples. Furthermore, this separation was that measured in Ag foil.

The coordination number was obtained from the analysis of the amplitudes. The amplitude $A_b(k)$ was analyzed by plotting $\ln[A_b(k)/A_{foil}(k)]$ vs k^2, where $A_{foil}(k)$ is the amplitude envelope of silver foil. The intercept of the curve gives $\ln[N_b/N_{foil}(R_{foil}^2/R^2)]$ where $N_{foil} = 12$ and R_{foil} is equal to the silver-metal nearest-neighbor distance at 78 K. The value of N_b obtained for the smallest particles was 11 ± 2, very close to the coordination of 12 for fcc silver. The analyses for the other samples with larger average particle sizes gave $N \simeq 12$. The coordination numbers obtained from the least-square fit of the data were always slightly smaller, for example, $N_b \simeq 8-11$ for the smallest average particle size. Because of the numerous factors appearing in the amplitudes [see Eq. (1)], we do not consider the variation in coordination number to be significantly different from the value for fcc silver.

DISCUSSION

The contraction observed for the smaller silver particles isolated in argon can be explained using the method developed by Vermaak, Mays, and Kuhlmann-Wilsdorf.[11,12] According to this work the surface stress can cause small spherical particles to be in a state of compression (for positive surface stress). There is experimental corroboration of the above statement.[2,3] If we use

this approach to analyze our results, we find considerable agreement between theory and experiment. For simplicity, assuming the particles to be spherical, one obtains the following relation[12] between surface stress, f, and P, the hydrostatic pressure due to the surface of radius r,

$$f = \tfrac{1}{2} rP . \qquad (2)$$

With the use of the relation for the compressibility $\kappa = -\Delta V/PV$, for a cubic crystal the following relation is obtained:[12]

$$f = -\frac{3}{2} \frac{\Delta a}{a} \frac{r}{\kappa} , \qquad (3)$$

where Δa is the change in lattice constant due to the surface stress. From the above-mentioned formula one can easily find the expected contraction in the nearest-neighbor distance[2]

$$\Delta R = -\frac{2}{3} f \frac{R_{Ag}\kappa}{r} . \qquad (4)$$

Using the values of $\kappa = 9.6 \times 10^{-13}$ cm²/dyn, $R_{Ag}(78$ K$) = 2.87$ Å (Ref. 17), and $f = 1415$ dyn/cm (as determined in Ref. 2), we obtain $\Delta R = 0.022$ Å which gives a value of $R_{NN} = 2.848$ Å, slightly larger than the value observed experimentally. However, we have used the value of f obtained by Wasserman and Vermaak[2] at 50 °C and assumed it to be valid at 4.2 K. Consequently, the small disagreement is not unexpected. We also must take into consideration that there is a wide range of values reported in the literature for f, from 6405 (Ref. 18) to 1415 dyn/cm (Ref. 2). If we use our value of ΔR to determine f, we obtain a value of 2286 ± 200 dyn/cm. In Fig. 9 we show the plot of R versus average particle size; the continuous line corresponds to the values predicted from the above model. There is very good agreement between experiment and theory. It should be pointed out that the interatomic distance for Ag_2 has been calculated utilizing the optical spectroscopy measurements[19] to be 2.5 Å. The contraction observed in our experiments points in the same direction. It seems that the simple equation given above can be used down to very small clusters. Other metals such as Cu can have very small surface stress values $(0.0 \pm 450$ dyn/cm$).$[3] In such a case one will not observe a significant contraction if it is primarily due to surface stress. Only when molecular sizes have been reached (a few atoms) will one observe a contraction.

The work presented here gives good evidence of the importance of surface stresses in causing a contraction of the interatomic distances for small silver particles. According to Orowan,[20] such a contraction occurs because $\partial\sigma/\partial e_{ij}$ is intrinsically negative for crystals (where σ is the surface tension and e_{ij} is the strain). [The surface stress is related to σ by the following relation: $f_{ij} = \delta_{ij}\sigma + (\partial\sigma/\partial e_{ij})$.] Our results are in full agreement with this model which predicts that the stress in the surface is a compression.

[1]R. P. Messmer, in *The Physical Basis for Heterogeneous Catalysis,* edited by E. Dranglis and R. I. Jaffee (Plenum, New York, 1975).

[2]H. J. Wasserman and J. S. Vermaak, Surf. Sci. $\underline{22}$, 164 (1970), and references therein. Here a good discussion of the possible errors in the analysis of the electron diffraction is presented.

[3]H. J. Wasserman and J. S. Vermaak, Surf. Sci. $\underline{32}$, 165 (1972).

[4]G. Apai, J. F. Hamilton, J. Stöhr, and A. Thompson, Phys. Rev. Lett. $\underline{43}$, 165 (1979).

[5]P. A. Montano and G. K. Shenoy, Solid State Commun. $\underline{35}$, 53 (1980).

[6]H. Purdum, P. A. Montano, G. K. Shenoy, and T. I. Morrison, Phys. Rev. B $\underline{25}$, 4412 (1982).

[7]E. P. Kündig, M. Moskovitz, and G. A. Ozin, Angew. Chem. Int. Ed. Engl. $\underline{14}$, 292 (1975).

[8]G. A. Ozin, Catal. Rev. Sci. Eng. $\underline{16}$, (2), 191 (1977).

[9]H. M. Nagarathna, P. A. Montano, and V. M. Naik, J. Am. Chem. Soc. $\underline{105}$, 2938 (1983), and references therein.

[10]H. Abe, W. Schulze, and B. Tesche, Chem. Phys. $\underline{47}$, 95 (1980).

[11]J. S. Vermaak, C. W. Mays, and D. Kuhlmann-Wilsdorf, Surf. Sci. $\underline{12}$, 128 (1968).

[12]C. W. Mays, J. S. Vermaak, and D. Kuhlmann-Wilsdorf, Surf. Sci. $\underline{12}$, 134 (1968).

[13]D. E. Sayers, E. A. Stern, and F. W. Lytle, Phys. Rev. Lett. $\underline{27}$, 1204 (1971).

[14]P. H. Citrin, P. Eisenberger, and B. M. Kincaid, Phys. Rev. Lett. $\underline{36}$, 1346 (1976).

[15]G. Martens, P. Rabe, N. Schwentner, and A. Werner, Phys. Rev. Lett. $\underline{39}$, 1411 (1977).

[16]P. A. Lee and G. Beni, Phys. Rev. B $\underline{15}$, 1862 (1977).

[17]Y. Pautamo, Ann. Acad. Sci. Fenn. Ser. A6: $\underline{129}$, 1/45, 33 (1963).

[18]C. R. Berry, Phys. Rev. $\underline{88}$, 596 (1952).

[19]M. D. Dolgushin, Opt. Spektrosk. Opt. Spectrosc. (USSR) $\underline{19}$, 289 (1965).

[20]E. Orowan, Z. Phys. $\underline{79}$, 573 (1932).